Deliverable 4.2: A final version of the final report

Prepared for:

New York State Energy Research and Development Authority

Albany, NY

and

The National Offshore Wind Research & Development Consortium

Albany, NY

Melanie Schultz
Program Manager

Prepared by:

GE Research

Niskayuna, NY

Project Manager 1: Guiju Song, PhD
Platform Leader – Offshore Wind at GE Research

Project Manager 2: Susan Kocsmiersky
Contract Administrator at GE Research

.

Notice

The New York State Energy Research and Development Authority (“NYSERDA”) and the National Offshore Wind Research and Development Consortium (“NOWRDC”) have not reviewed the information contained herein, and the opinions expressed in this report do not necessarily reflect those of NYSERDA, the State of New York or NOWRDC.

This material is based upon work supported by the U.S. Department of Energy’s Office of Energy Efficiency and Renewable Energy (“EERE”) under the Wind Energy Technologies Office Award Number DE-EE0008390.

This report was prepared as an account of work sponsored by an agency of the United States Government, NYSERDA and NOWRDC. Neither the United States Government nor any agency thereof, NYSERDA or NOWRDC nor any of their employees, makes any warranty, express or implied, or assumes any legal liability or responsibility for the accuracy, completeness, or usefulness of any information, apparatus, product, or process disclosed, or represents that its use would not infringe privately owned rights. Reference herein to any specific commercial product, process, or service by trade name, trademark, manufacturer, or otherwise does not necessarily constitute or imply its endorsement, recommendation, or favoring by the United States Government or any agency thereof, NYSERDA or NOWRDC. The views and opinions of authors expressed herein do not necessarily state or reflect those of the United States Government or any agency thereof, NYSERDA or NOWRDC

GENERAL ELECTRIC COMPANY MAKES NO WARRANTY OR REPRESENTATION, EXPRESS OR IMPLIED, AS TO ANY MATTER WHATSOEVER WITH RESPECT TO THIS DOCUMENT, AND SPECIFICALLY DISCLAIMS ALL WARRANTIES, INCLUDING, WITHOUT LIMITATION, ANY WARRANTY REGARDING THE ACCURACY OR PERFORMANCE OF THE DELIVERABLES OR WORK, THE DESCRIPTION, FITNESS, OR SUITABILITY OF THE DELIVERABLES OR WORK IN ANY RESPECT OR IN CONNECTION WITH OR FOR ANY PURPOSES OR USES, THE DURABILITY, QUALITY, OR CONDITION OF THE DELIVERABLES OR WORK, THE NON-INFRINGEMENT OF ANY INTELLECTUAL PROPERTY RIGHTS, THE COMPLIANCE WITH REGULATORY REQUIREMENTS, AND THE MERCHANTABILITY OF THE DELIVERABLES AND FITNESS FOR A PARTICULAR PURPOSE.

Table of Contents

List of Figures

Acronyms and Abbreviations

DOE	Department of Energy
NOWRDC	National Offshore Wind Research and Development Consortium
NYSERDA	New York State Energy Research and Development Authority
PAB	Project Advisory Board
PM	Program Manager
PI	Principal Investigator
LCOE	Levelized Cost of Energy
SOW	Statement of Work
O&M	Operation and Maintenance
POC	Proof of Concept
USV	Unmanned Surface Vessel
ROV	Remotely Operated Vehicle
UAV	Unmanned Aerial Vehicle
GCS	Ground Central Station
GPU	Graphics Processing Unit
DNN	Deep Neural Network
AUV	Autonomous Underwater Vehicle
ASV	Autonomous Surface Vessel
PC	Positioning Camera
TC	Tracking Camera
FOV	Field of View
COTS	Commercial-off-the-shelf
PTU	Pan and Tilt Unit
RGB	Red, Green, and Blue
PSO	Protected Species Observers
HDMI TX/RX	HDMI Transmitter/Receiver
SAM	Segment Anything Model
CNN	Convolutional Neural Network

Executive Summary

Over the next decade there will be an order of magnitude increase in the number and complexity of installed offshore wind turbines in US waters. This growth presents an opportunity for technology advancement to reduce the 30% Operations and Maintenance (O&M) contribution to the Levelized Cost of Energy (LCOE). This project aims to advance the remote inspection and monitoring technologies and strategies for exterior components of offshore wind turbines, in turn, to reduce the O&M cost for offshore wind. This program focuses on the design and development of an autonomous multi-sensing system, capable of inspecting fleets of turbines with minimal to no operational interruption, operating over a wide region while at-sea for long duration missions. This will be accomplished by transferring advanced inspection and monitoring technologies from onshore to offshore wind while solving the complex challenges of collecting high-quality data at varying operation conditions (e.g., sea states)

This project includes four technology development tasks:

Task 1 is about the conceptual design of the multi-sensing system. The team has created a conceptual design of a proof-of-concept (POC) multi-sensing system for use in conjunction with autonomous vessel-based inspection of offshore wind turbines, with the design specifically focusing on the strategies for data quality enhancement. A list of system requirements and specifications for a conceptual design was first defined based on a complete vision of an autonomous vessel-based inspection system. A collection of subcomponents was down selected and assembled to build a POC imaging system. And then the POC imaging system was integrated with a commercial unmanned surface vessel (USV). The summary of the technology development and results for Taks 1 was reported in Section 2 and 3.

Task 2 is about the lab-based feasibility study on low-latency image acquisition control. The team studied the feasibility of the low-latency image acquisition control with advanced analytics with the purpose to improve data collection quality. Particularly, a small-scale lab set-up was developed so a tracking and positioning camera duo and an AI based turbine detection software pipeline were adopted to detect the blade position and calculate the rotating speed. Consequently,

the blade of interest was accurately positioned and captured in the center of the imaging camera field as high-quality inspection data. The summary of the technology development and results for Taks 1 was reported in Section 6.

Task 3 is about the data quality assessment with autonomous vessel. The team has completed two sub-tasks. In Subtask 3.1, the team conducted two rounds of testing with the integrated vessel at the Mystic River as a simulating setting and in the Block Island wind farm as the real ocean environment. The objective of the testing was to collect data and validate the system functions and capabilities in various environmental conditions. During the data collection, the team has been working closely with a 3rd party to observe environment impacts and avoid strikes in the ocean. In Subtask 3.2 (assess and enhance data quality), a thorough data assessment on images collected in Subtask 3.1 has been conducted to estimate the image resolution, sharpness, and quality for defect detection. Our research proved that the designed USV based-, imaging system is capable of capturing high quality offshore wind blade images in a real wind farm. The summary of the technology development and results for Taks 3 was reported in Section 4 and 5.

In summary, our research effort in this project has built and proved a design comprising a USV, a dual camera combo, and an AI based software pipeline can conduct offshore wind blade inspection when turbines are operating although the POC studies for the USV based- imaging system and the low latency blade tracking system were conducted separately. In the potential future phases of the project, the team will integrate the two above-mentioned systems to one, demonstrate its functionalities at a full scale and in a ruggedized configuration, and ultimately advance the USV based- autonomous inspection technology for offshore wind to commercially ready.

1 Project Introduction and Objective

1.1 Project Background

Global offshore wind capacity reached to 27 GW in 2019 [1] with projection to 215 GW or more by 2030 [2]. While in the U.S., the Biden Administration announced a target to install 30 GW of capacity by 2030 [3]. With the Operation & Maintenance (O&M) contributes approximately 30% of LCOE [4], the yearly cost of O&M globally will increase from $5B to more than $25B [5]. The current available inspection and monitoring strategies for offshore wind are either cost prohibitive or limited by varying offshore operational conditions such as weather and sea states. These existing inspection technologies typically require technicians onsite, and the wind turbines often needs to stop operations for human operators to conduct the inspections. These increase the labor hours spent at sea, increase the safety risk, and decrease turbine availability due to downtime.

On the other hand, advanced O&M sensing strategies and analytics have been developed and field-validated in the onshore environment for wind turbines monitoring and inspection. However, there are significant challenges in applying these mature onshore technologies to offshore wind turbines. It is often challenging to directly apply the sensors that collect data of exterior turbine components of onshore to those of offshore wind, due to the varying sea conditions. For those inspection technologies that have been applied to the offshore world, there is a challenge of acquiring and analyzing high-quality data at sea in a technically and economically scalable way. For example, aerial drone-based technologies are available commercially for offshore turbine inspections. Due to limitations in drone payload and endurance, they are however cost prohibitive for long-term monitoring and inspections of large number of offshore turbines. Autonomous drone inspection has been demonstrated in the past. However, majority of the current drone inspection offerings need operators nearby due to regulatory constrain, and require turbine to halt operation, which leads to reduced turbine availability. Hence, there is an opportunity to develop a multi-sensing system to conduct robust inspection at varying sea conditions. Such system can enable adaptation of proven technologies from onshore wind to offshore, advance offshore O&M strategy, reduce LCOE, and accelerate the U.S.'s ability to economically deploy offshore wind technology.

1.2 Related Work

The offshore wind power industry is an emerging and exponentially growing sector as it is expected to be one of the main sources of energy in a near future [6] [7]. The increase in the development of this type of facilities calls for a cyclic inspection routine to ensure their safety and efficiency. Under the current technological base, inspection tasks are labor-extensive, dangerous, and highly influenced by environmental conditions, and are mostly carried out by using Remotely Operated Vehicles (ROVs) and divers [8].

1.2.1 Inspection using aerial vehicles

Unmanned aerial vehicles (UAVs) have been widely used to inspect wind turbines at a regular basis, improving its maintenance. The number of aerial inspections performed by UAVs have grown significantly over the past few years due to the improvements in inspection quality in comparison to the use of conventional operator-based inspections [9, 10]. The quality of an inspection depends on multiple factors, such as quality of image, its resolution, lighting conditions, and information about damage severity, among others. The output of a successful wind turbine inspection is a collection of images that include detailed description of the damage including its approximate location and size, extent, and the cause of damage, e.g., rain or sea water erosion, bird strike, lightning strike, etc.

There is extensive literature on drone-based inspections [11, 12, 13, 14]. The quality of photos and videos taken by using such airborne vehicles is strongly influenced by vehicle motion induced by environmental conditions, which in turn, affects the quality of the data and hence, the degree to which damages can be identified. The cost of carrying an onboard camera affects the battery performance significantly, which limits the drone’s flight-time. Hence, drone-based inspections are not extendable to large-scale power projects.

In most existing work, we observed that photographs taken by drones operated manually often have low resolution due to the onboard battery limitations. Moreover, the drones are operated from a considerable distance from the turbine to maintain safety for the drone. This leads to the turbine blades appearing very tiny in the images and damages become difficult to detect. In [15], Løhndorf et al. developed a pinhole camera model to estimate the image pixel size and estimate the sizes of objects through pixel counting. Using their method, photographs taken by an UAV were used to estimate the size of several features with relatively high precision, while maintaining a safe distance from the wind turbine. However, the resolution of the LiDAR used in this work prevents the model from measuring important parts of a wind turbine structure, such as wing tips and trailing edges.

In [16], Durdevic et al. proposed a control system for an autonomous drone for inspection of wind-farm turbines. Their prototype model employed a distributed architecture consisting of a Ground Control Station (GCS) that performs the heavy computations using a high-performance GPU required for training and inference of a Deep Neural Network (DNN). A client onboard the drone would send images from the camera and receive a probabilistic estimate of the existence of a wind turbine in the images. However, this approach has a bottleneck in reducing the level of autonomy of the drone and requires a high-bandwidth wireless connection to send the images from the client (drone) and to receive commands from the GCS.

1.2.2 Inspection using marine robotics

Unlike aerial or ground robots, where the environment is usually bounded by the ground plane, in marine robotics the same scenario presents two different domains depending on the operability in regions divided by the water surface. The different constraints on the sensor availability and mapping techniques for autonomous marine vehicles, both below and above the water surface, demand distinct approaches to marine robotics. These constraints define the different domains of marine robotics, namely immersed using ROVs and Autonomous Underwater Vehicles (AUVs), and emersed using Autonomous Surface Vehicles (ASVs). Attempts have been made to merge the visual data accumulated from these two platforms [17, 18] showing promising results.

In [19], Pinto et al. developed a maritime testing platform called ATLANTIS that allows the demonstration of key enabling robotic technologies for inspection and maintenance of offshore wind turbines. The test platform consists of two separate testbeds: 1) a Coastal Testbed equipped with a monopile and a floating structure system, as well as an onshore control room, from which all tests are monitored; and 2) an Offshore Testbed consisting of dedicated positions within a commercial wind farm that is reserved for demonstrating robotic technologies in a real environment. Platforms like ATLANTIS have promoted the development and testing of more marine robotic technologies such as the one described by Campos et al. in [20].

1.2.3 Interior inspection of wind turbines

Structural components of a wind turbine may be produced with manufacturing defects [21], but also suffer from constant damage due to environmental changes while in operation [22], especially the blades that are commonly affected by bird or insect strikes [23], lightning strikes [24], accumulation of ice and dirt, corrosion due to saltwater [25], or erosion due to rain or small dirt particles in the wind [26]. Manned interior inspections can be carried out by trained technicians who use specialized tools to move around and inside the turbines to perform tests using inspection tools such as ultrasound, radiography, or thermography [27]. For interior inspections, crawler robots have also been used [28].

1.3 System Requirements & Key Design Parameters

Inspection is an increasingly critical process in the O&M of an offshore wind turbine. The quality and fidelity of the data acquired during inspections has profound downstream consequences on decisions such as how to operate and when to repair the wind turbine. The acquisition of high-quality data has become a focal point of wind turbine O&M and forms the thrust of this work.

Data acquisition typically falls into two categories: 1) contact-based or local inspection, and 2) standoff inspection. Local inspection requires that the data acquisition system be carried up the tower and placed (usually by a human inspector) in close proximity or in contact with the component being inspected. Ultrasound, acoustic tap test, and internal visual inspection fall into this category. The nature of these inspections requires a human to travel to and climb the tower, and sometimes entering the confined space of the hub and blades. The expense of this activity puts a limit on the frequency and quality of the data being acquired.

Standoff inspection is the second category of inspection and is usually done at a distance, e.g., either from an aerial vehicle or from the ground. The requirement for a human to arrive onsite and to climb the tower are substantially lower and may be removed altogether via automation such as autonomous aerial drones. This type of autonomous data acquisition has been under heavy development for more than a decade and many times is the primary mode of inspection before a more thorough human-based inspection is required. The cost of this type of automated data acquisition for land-based turbines can be an order of magnitude cheaper than the contact or local equivalent inspection and has become the dominant form of inspection for onshore wind turbines.

When building a standoff sensor data acquisition system for offshore wind turbine, the choice of a sensor modality depends to a great extent on what indication (evidence of a defect) is required for defect identification and characterization. For this program, each sensor modality requires an understanding of the impact of several system requirements and key design parameters, including resolution, targeting accuracy, coverage, and environmental requirements. We discuss each of these for both visible light and infrared thermography below. Visible light cameras for example are used extensively to provide indications of damaged bearings (liberated grease), damaged blade exterior such as cracks, erosion, and scorching due to lightning damage. Infrared thermography can be used to detect substructural heating and cooling to indicate excessive bending or structural damage such as internal cracks and delamination.

- **Resolution**: typical resolution requirements are expressed as pixel density on target or smallest resolvable feature. Both are important but for this work we will focus on pixel density. Our working specification is 1 Pixel/mm, which is comparable with the equivalent drone visual inspection for onshore turbines. Similarly, for infrared thermography the pixel density is roughly 2 pixels/mm^2.

- **Targeting Accuracy and Coverage.** These two specifications work in tandem to allow for the complete and accurate acquisition of the entire targeted area. Again, we turn to the drone-based inspection requirements to derive our preliminary system requirement. The data acquisition system must be able to point the camera with enough precision and stability to reliably acquire the entire blade surface over the course of the inspection. Doing this offshore without the possibility for remote control requires that we develop a targeting system tolerant to the communication lag associated with offshore vessels. Lack of cellular coverage and the cost of direct satellite communication requires the need of an intelligent targeting system capable of data acquisition without direct human control over long missions for many turbines.

- **Environmental Requirements** provide the greatest challenge for the offshore automated data acquisition system. Varying sea conditions demands the use of a stabilization system such that the camera can be reliably pointed to the target interest while rejecting vibration, roll, and pitch of the vessel. This system must work with the targeting system to ensure high quality data is acquired. Additionally, the nature of the offshore environment will require the ability to deal with sensor fowling by the marine environment as well.

1.4 Project Objective

This project aims to advance the remote inspection and monitoring technologies and strategies for exterior components of offshore wind turbines. This will be accomplished by transferring advanced inspection and monitoring technologies from onshore to offshore wind while solving the complex challenges of collecting high-quality data at varying operation conditions (e.g., sea states). The project has been focused on designing, developing, prototyping, and testing an unmanned surface vessel (USV) based- imaging system. The objective is to prove this system could meet the system requirements mentioned in Section 1.3 and generate high quality images serving as a novel solution for the offshore wind inspection.

2 System Conceptual Design

In order to capture images of the wind turbine blades and components with the required resolution specified in Section 1.3, the image capturing system must be able to operate semi-autonomously on the surface vessel, with only periodic communication with the control center via the high-latency link. Figure 1 shows the overall system architecture of the proposed imaging system. It consists of camera/s stabilized by a gimbal to capture images at the front-end. The back-end components consist of local storage and software modules that performs image processing and recognition, as well as turbine and blade tracking algorithms. A long-range or satellite wireless module will also be included for receiving parameters of targeted wind turbine models, and for uploading captured images when necessary. In what follows, we present three different potential options to achieve the purpose.

Figure 1. Overall System architecture.

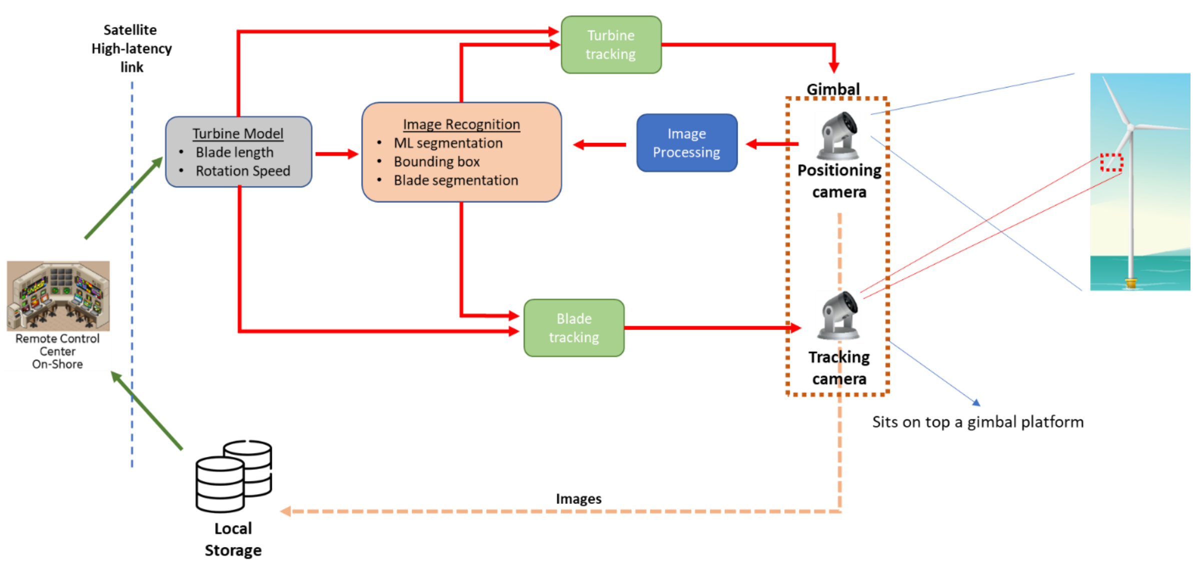

Option 1 (Figure 2) employs two cameras, namely the Positioning Camera (PC) and the Tracking Camera (TC), both stabilized by a gimbal platform. The PC is equipped with a wide-angle lens and is responsible for ensuring the whole wind turbine is always in the camera's field of view (FOV) during image capture operation. This allows the image segmentation module to estimate the rotational speed of the blades across multiple frames. Fusing that with the wind turbine's

parameters, future positions of the individual blades within the FOV of the camera can be predicted.

Figure 2. Option 1 of two cameras with spiral motion tracking path.

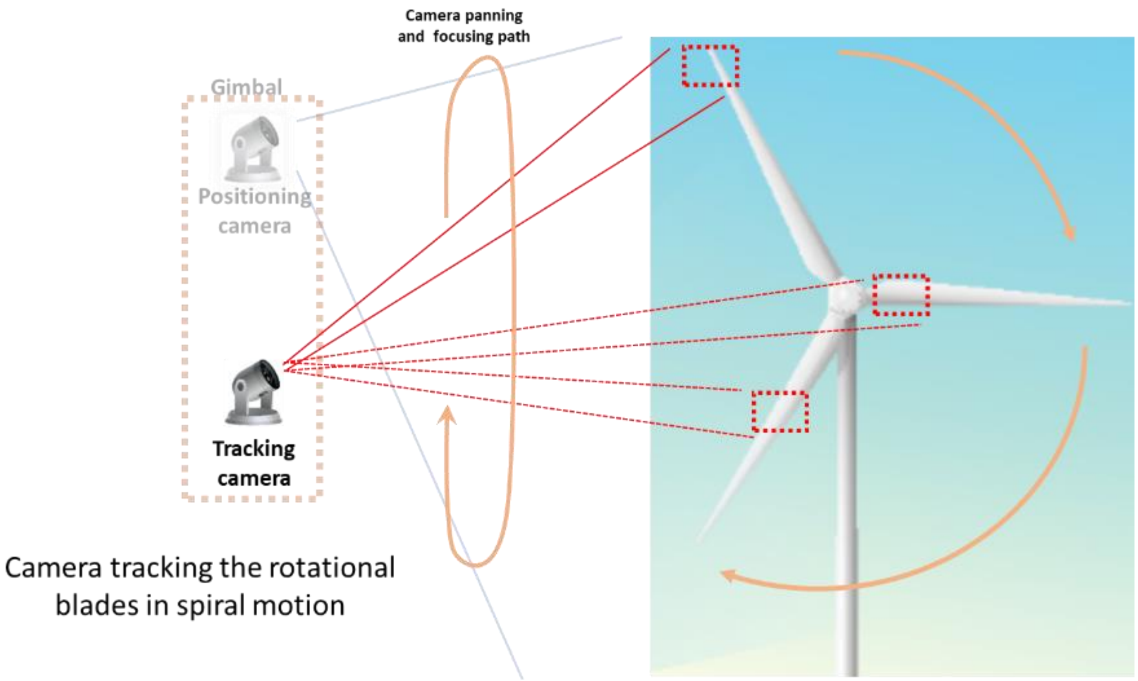

The TC is equipped with a telephoto-lens that can zoom and capture close-up, high-resolution images of different sections of a blade. With a fixed, static physical configuration between the PC and TC, the predicted positions of the blades within the PC's local frame can be transformed onto the TC's local frame.

The blade rotational information allows the TC to perform visual servoing to track each individual blades and take high-resolution images from the root to the tip of the blade in a spiral motion.

Similar to Option 1, Option 2 (Figure 3) consist of both the PC and TC for turbine blade image capturing. The PC is equipped with wide-angle lens and functions as spotting camera to ensure the entire wind turbine in its FOV. Instead of tracking the rotational motion of the blades in a spiral fashion, the TC capture blade sections in a straight path, from the tip to the root of the blade. Since the wind turbine continues to operate, the target blade section will only be within the FOV of the TC once per turbine revolution. In order for the TC to capture images of the blade while it is rotating, precise timing of the blade rotation is critical. This information can be estimated by the fusion of the rotational speed estimation of the PC and the wind turbine parameters provided by the operator.

Figure 3. Option 2 of two cameras with fixed tracking path.

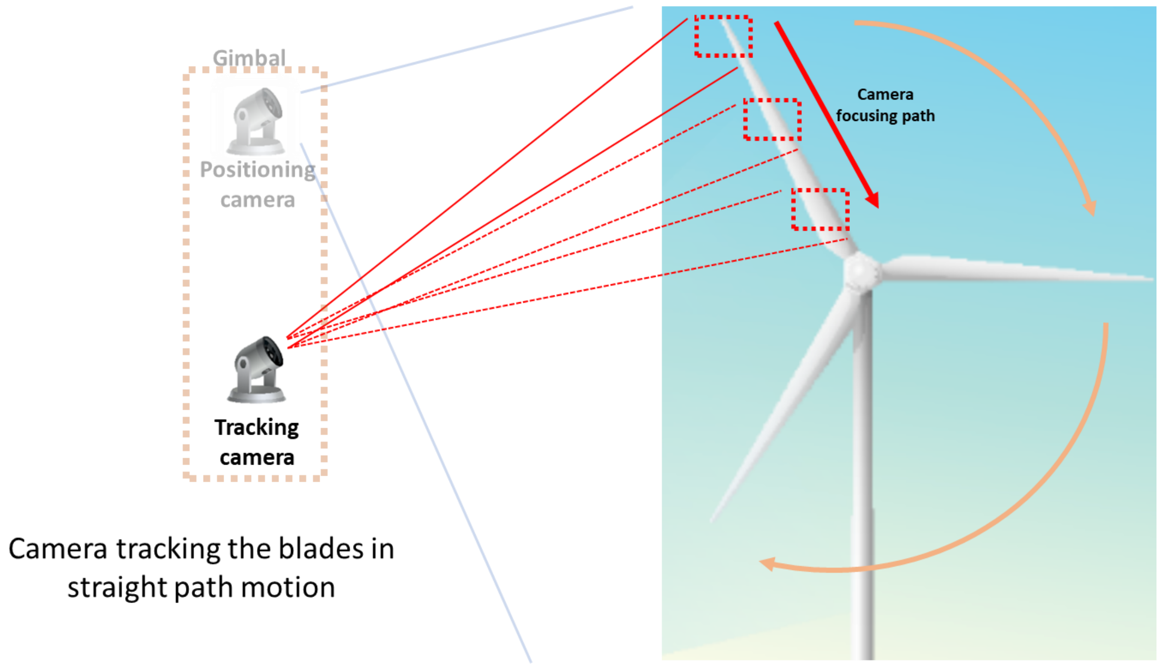

Option 3(Figure 4) relies only on a single high-resolution camera, while eliminates the need for the spotting camera for the estimation of the wind turbine rotational speed. The idea is to ensure that the entire wind turbine is within the FOV of the high-resolution camera while images are being captured. During post-processing, zoomed-in sections of the blades will be cropped out from the captured images for defect recognition and inspection. This approach only requires the gimbal to stabilize a single camera as it locks its focus on the wind turbine.

Figure 4. Option 3 of a single, high-resolution camera.

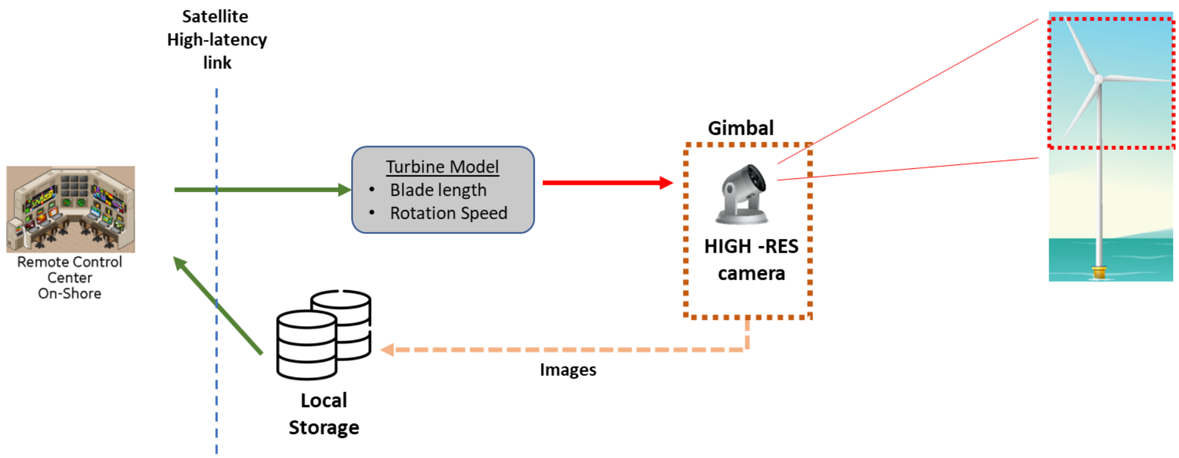

Different approaches presented have their respective advantages and disadvantages. Option 1 and 2 require two camera systems and precise inter-camera coordination to perform both wind turbine spotting and tracking. However, this approach allows the tracking camera to zoom in onto the blade section of interest and capture high resolution images while the wind turbine is operating.

Option 1 allows the blade section of interest to be always in the FOV of the tracking camera, thus, increases the chance of capturing sharp images with minimum motion blur since the tracking camera is panning in a spiral motion, in-sync with the rotational speed of the turbine blades. However, this also requires continuous actuation of the pan-tilt unit during the operation, thus increases the hardware wear and tear, or failure.

On the other hand, Option 2 depends heavily on good estimation of the rotational speed of the wind turbine and the ability to trigger the tracking camera's shutter at precise timing when the blade section of interest moves within the FOV of the camera. In order to avoid motion blur, high shutter speed setting would be required. This could potentially limit the operation envelope of the proposed system due to the requirement for brighter condition to compensate the high shutter speed setting of the camera.

Option 3 has the advantage of system and operational complexity, since only a single camera is used for capturing images of wind turbine blades, and there is no spotting or tracking required. Once the camera has its focus locked on the wind turbine, images of the entire blade can be captured continuously. In order to capture good quality, still images of the rotating blades, the camera high shutter speed and high aperture setting to maximize image sharpness and minimize motion blur especially at the tip of the blade where the relative velocity is the highest. Furthermore, the camera must have a high-resolution, low-noise sensor, such that the cropped-out sections of the blade section of interest has enough pixel density for effective defect detection.

To prove the conceptual design(s) can provide high quality images sufficient for offshore wind blade inspection, the team has completed the proof-of-concept prototype development and test for two separate systems. One system was the USV based cameral system capable of capturing high quality images in the ocean environment as described in Section 3, 4 and 5. Another one was a lab based- blade tracking system (Section 6) capable of monitoring the blade position in real time and controlling the inspection camera’s FOV to cover the object of interest (wind blade).

3 System Integration and Prototyping

This section will summarize the proof-of-concept-, USV based- cameral system capable of capturing high quality images in the ocean environment. We will describe the system configuration first, the component selection for such a system as next, and then the overall system integration. The function and performance testing in the lab environment will be reported in Section 3.2.

3.1 POC System Configuration

The focus of the section was to define the proof-of-concept system configuration including an autonomous vessel carrying inspection subsystems, imaging systems for inspection data acquisition, and a crew vessel to safeguard the autonomous vessels in case of unexpected malfunction during the test, as well as serving the purpose of strike avoidance of endangered species. The team has defined a schematic and integrated system shown in Figure 5 below.

Figure 5: Schematic and integrated system for field data acquisition and system testing.

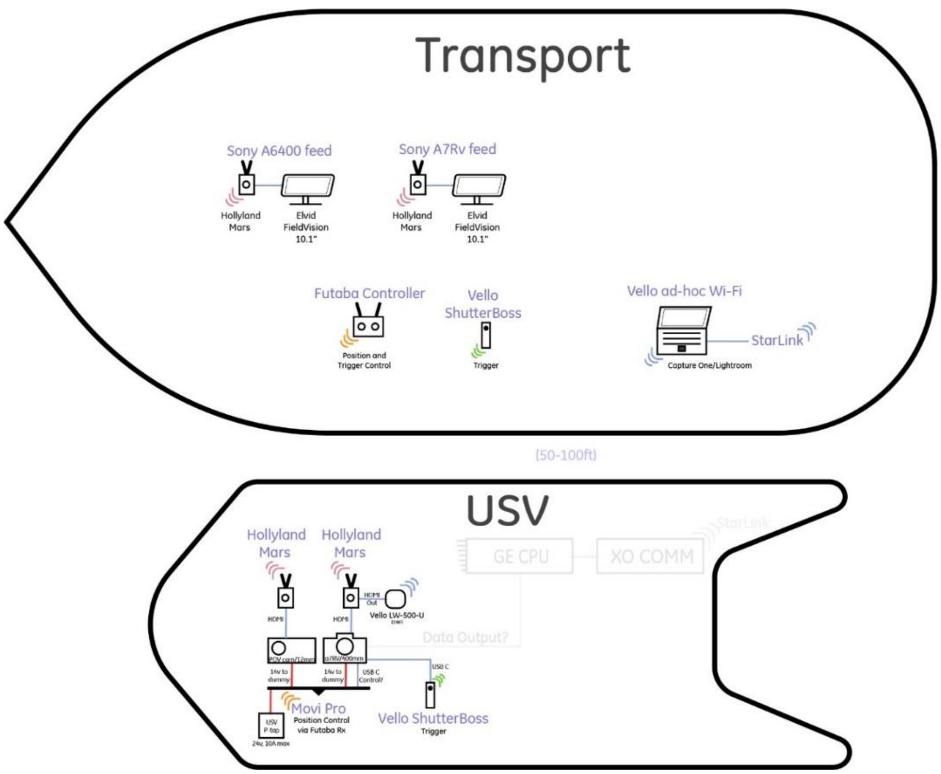

The system is comprised on a plethora of subsystems including a crew transport vessel and an USV by XOCEAN, our vessel vendor, to perform the remote inspection task. The core component of the USV system is a three-axis FREEFLY MōVI gimbal. The gimbal and subsystems will be powered via a 24v DC power tap provided by the XOCEAN USV. The gimbal will house the two cameras (data acquisition camera and a positioning camera), dual Hollyland HD video transmitters, Futaba remote controller receiver, Vello wireless data transmitter, and a camera shutter intervalometer.

3.1.1 Criteria for Camera System Down Selection

Finding a capable imaging system for the watercraft was critical to the project success. The team has defined a set of selection criteria for the camera system listed below:

- Scaled and weighted such that it can be mounted on a small, unmanned sea vessel
- Of sufficient resolution to detect defects at 50~100-meter distance
- x/y positioning capability to dampen waves at a normal sea state, and targeting rotating wind turbine blades
- Capable of being protected from environmental conditions, such as salt, water, wind, sun, etc.
- Having a control system commensurate with the positioning system (refer to technical report Deliverable 1.1)
- Cost effective with reasonable lead time (e.g., 2 months)

Evaluation of optional systems was focused on three main areas: current offshore imaging systems, security-based camera systems, and videographer/film-based systems.

Through some evaluations and comparisons of commercially available solutions across industries, we have concluded that it is less likely to find a readily available commercial-off-the-shelf (COTS) solution that meets all the program’s technical and budgetary criteria, and a custom solution developed and integrated with COTS components will be most likely required as a commercial product or service offering. To test the feasibility of the proposed system, we will procure COTS components to build out a proof-of-concept system that would allow us to test in the field with appropriate level of development effort to make it environmentally rated and automated from a control perspective.

3.1.2 Camera Selection

The imaging system we selected is twofold. For the long-range data acquisition, we will use a Sony a7R V 61MP camera with a 400mm lens shown in Figure 6. For positioning, a much wider field of view camera is selected.

Special consideration is made in the mounting of the large camera and lens combination as the weight and scale of the lens is unusual for normal gimbal operations. Mounting the camera such that proper gimbal balance is maintained will require extended mounting plates, lens supports, a camera cage, as well as weights on the back side of the camera.

Figure 6: Long-range data acquisition camera (Sony a7R 61MP and 400mm lens).

For the positioning camera, we will use a lightweight 1080P 60fps AIDA camera shown in Figure 7.This will allow us to maximize the capability of, and lessen the strain on, the gimbal due to its small form factor (1.5”x1.5”x2”). This camera will be used for a live feed only, and no data will be recorded wth it.

Figure 7: Wide-angle positioning camera (AIDA 1080P).

3.1.3 Image Stabilization Subsystem

After evaluating many different pan/tilt and gimbal options, we have selected the FREEFLY MōVI gimbal for its cost, overall scale, payload capability (12lbs), remote power modification ability (gimbals normally use batteries) and flexibility with respect to camera and lens mounting options. The gimbal will work to effectively reject the motion of the waves in all directions (except Z/*vertical*, which will have little effect on positioning accuracy) to reduce operator effort on aiming accuracy.

Since we are on a moving platform and the 400mm lens we choose for the POC system is quite long with a mere 6° FOV, it will be difficult to always stay on target. Once the user loses their positioning on the blade, typically only sky will appear with no distant and distinct reference points. Therefore, it is necessary to have a frame of reference for where we need to aim (e.g., left, right, above, below) with respect to the blade section of interest. We choose to use a positioning camera with a much wider FOV than the data acquisition camera, such that the operator may glance at the position camera remote screen and decide on a direction to adjust the gimbal in the case of target loss from the data acquisition camera. For the operator, dual monitors will be placed side by side, and embedded aiming crosshairs will facilitate targeting. When mounting the two cameras on the gimbal, we will align them vertically, and aim them at a point centrally, about 100m away.

To control the gimbal, a dual stick Futaba controller will be used to allow the operator to adjust the pan, tilt and roll capabilities of the gimbal. We may be able to integrate the shutter via the controller as well and avoid the use of an intervalometer, but this is to test and develop as needed in the next step. The controller also allows us to remotely fine tune the speeds and mapping of each individual axis on the gimbal.

3.1.4 Communication Among Subsystems

Each camera has an independent Hollyland video transmitter (Figure 8) feeding dual HD receivers and monitors on the Transport vessel. The Hollyland Mars Tx/Rx systems were chosen for their robust capabilities at a low cost. They have a 450’ range, automatic 5.8GHz channel hopping, very low latency of .06ms, a wide DC input range of 6-16v DC, ability to cross-convert SDI to HDMI and small form factor.

Figure 8: Wireless video transmitter.

There is an additional Vello transmitter (Figure 9) that we will attempt to tether to a laptop on the Transport vessel via its ad hoc WiFi network and Capture One software. With this stretch engineering task, we hope to acquire data in near real time, and stream them potentially via a Starlink uplink remotely, instead of waiting to retrieve the data when back at the docks several hours later via the SD card.

Figure 9: Wireless data transmitter (optional).

3.2 System Prototyping and Lab Test

Figure 10 is the bare gimbal system that will be mounted on the vessel using a quick release fitting, and custom mount on the XOCEAN vessel using standard 80/20 materials (1”x3” extruded aluminum base).

Figure 10: MōVI stock gimbal system and custom 80/20 mount

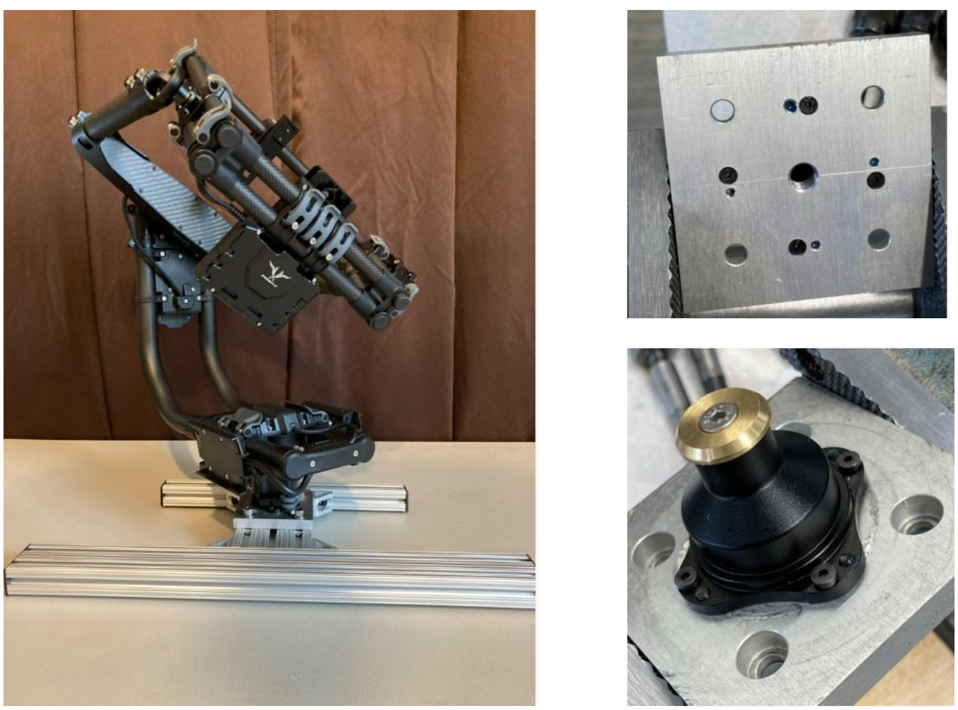

The integrated imaging system including two cameras and gimbal controller is presented in Figure 11.

Figure 11: Integrated imaging system

The dual wireless video transmitters shown in Figure 12 provide 1080p video signals back to the crew vessel. Live video will be displayed on the two screens. Our researchers on the crew vessel will monitor the videos in real time to ensure the blade being inspected is within the field of view, and that the image quality is acceptable. All other subsystem components were described in Deliverable 1.3.

Figure 12: Live video transmission and display

The system was assembled, and several technical issues were observed and mitigated during the buildup.

Gimbal performance and sensitivity

We are currently at 22 lbs of equipment, including the mounting base (3.25 lbs) and gimbal (5.84 lbs) which is rated for 15 lbs loads. Our added equipment weighs 12.91 lbs. When considering the added weight of the coiled power cable and its drag, we are very near the mechanical limits of the gimbal. Great efforts were made to position the heavy camera/lens combo such that minimal balancing weights were necessary to keep the overall system weight as low as possible. During testing, we observed gimbal motor interruption and overheating and concluded that balancing of the gimbal is more critical than on other gimbals, but observed to be working well once the system was balanced (showed in Figure 13) and tuned.

Figure 13: Spherical counterbalance weights required to balance offset lens weight

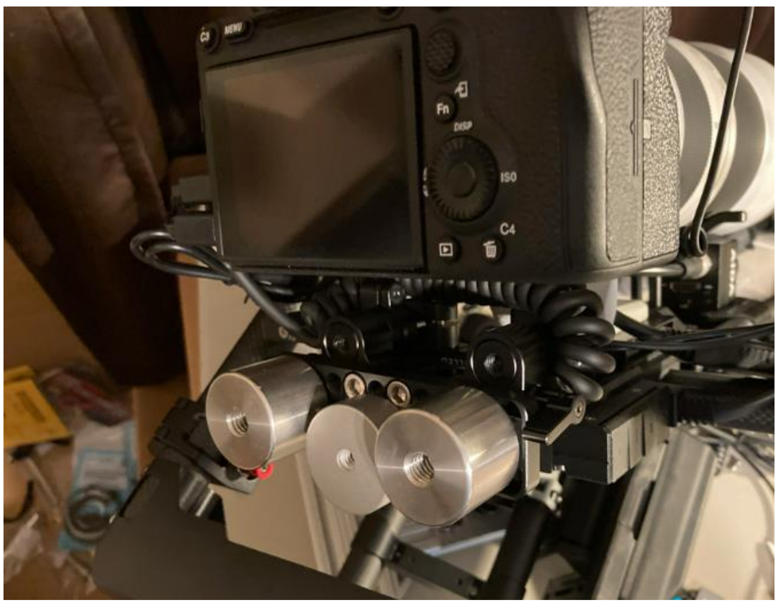

Cable management

As we are intending to power the gimbal from the XOCEAN vessel, we need to make a physical power connection to the rotating gimbal battery mounts. We could have used a large slip ring for power, but this would have added additional development time and significant costs. Based on a rated 24 VDC and 13 A max load, we chose a 16ga coiled cable at 2’ compressed length (about 2x length extended). Although the cable is quite bulky and will require careful cable management to avoid being tangled (See Figure 14), it is the simplest option. We repurposed a stock MōVI battery adapter, plugged it into one of the two available battery mounts, disassembled and wired the power cable into it and ran it to a power supply to observe max current draw under load. At idle, the gimbal and sub systems draw just 1.048 amps, however when an individual gimbal motor is loaded, we saw a fast rise of ~2.6 A. The gimbal motors have a protection mode when ~3 A is exceeded, as with the condition where the power cable is limiting movement. When considering that all three gimbal motors can fire simultaneously under heavy roll/pitch/yaw corrections, we can see why the gimbal can draw up to 13 amps, which also accounts for loads encountered by the communication and onboard charging systems for the camera batteries.

Figure 14: Power connection, video transmitters, battery and DC source power indicators

We also observed under a stress test that under the highest loads, it was possible to draw enough current quickly enough that the power supply could not keep up. As we cannot guarantee that the XOCEAN vessel can provide sufficient loads at this point in the project, we opted to retain one battery onboard the gimbal to smooth out any heavy draws the gimbal may have. Under normal operating conditions, the gimbal will draw from the supplied cable, but the battery provides a nice redundant backup power source (1-1.5 hours of run time). The gimbal is designed to dynamically flip from source to source without interruption to operation.

Wireless channel interaction and separation

Once the power was stable, we started to evaluate wireless performance. The transmitters are rated for 450 feet, but in testing, we observed just about 75 feet before starting to see signal dropout. We were aware that the proximity of the two transmitters on the gimbal and crew vessel were not ideal, but we do not have flexibility on the gimbal side to separate the two. But we did separate the crew vessel receivers by 8 feet and saw ~50’ improvement in solid transmission quality. Additionally, a wireless scan was performed, and it was observed that by choosing channel 1 on one TX and channel 8 on the other, another 50-100’ of range was observed – more than sufficient for the test. Additionally, in the lab environment, multiple 2.4GHz Wi-Fi and other networks may be impacting signal strength/quality, and these disparate signals are unlikely be present on the water. We will verify wireless performance later during the actual XOCEAN integration and testing phase.

Control

We opted to use a surface-rated Futaba stick controller. We were able to use a specialized control cable to connect the Futaba receiver to the gimbal to provide PTZ control. After some configuration, we were able to logically control the gimbal via the remote viewing screens. (Up on the stick pans the image up, left moves left, etc.). Additionally, we can select any gimbal speed via a rotating knob, or quickly flip between high and low speeds which is useful to get onto target quickly via the positioning camera, and then slow down the speeds to precisely position the inspection camera on an area of interest.

We had hoped to additionally use a switch on the Futaba showed in Figure 15 to trigger the inspection camera, but this is not possible within the MōVI gimbal as hoped, and although custom options exist for RC PWM to Sony shutter control via USB, we just opted to use a standard wireless intervalometer and during testing, which worked admirably. It allows us to pre-focus the camera via a half press of the shutter button before firing. The separation of the controller and shutter also allows multiple operators to split inspection duties.

We also will be evaluating the integration and performance of the Vello wireless transmitter which will symbiotically allow us to stream image content remotely from XOCEAN to the crew vessel, but with the trigger being initiated from an iPad touchscreen interface over Wi-Fi, we have concerns over latency and general HMI usability. We need to be able to accurately fire the camera if, for example, the turbine is pin wheeling, or the gimbal is not sufficiently dampening wave movement.

Figure 15: Futaba T4GRS radio and intervalometer

Remote viewing

A standard directors monitor cage was repurposed as a crew vessel viewing station. One receiver shown in Figure 16 is mounted to the rear of the cage, and a second receiver in Figure 16 is mounted 8’ away (an adjustable clamp will be provided to mount to a solid feature on the vessel).

We will use a red grid on the wide-angle positioning camera (left) to get a general field of view which provides a good way of getting the inspection camera (right) on target. Without the positioning camera, the inspection camera operator would have no situational awareness of where they are aiming.

Figure 16: Director's view

4 Field Testing

This section summarizes the two rounds of the field testing for the integrated system containing the USV and the imaging system prototyped in Section 3.2. XOCEAN's USV was shipped to GE's Niskayuna site in August of 2023. The team worked together to integrate the imaging system shown in Figure 11 with the USV. An integrated system is shown in Figure 17. As stated in the original proposal, this project aims to design and prove that a USV based- imaging system is capable of taking high quality images as a means of offshore wind blade inspection when turbines are operating. A blade tracking technology to enable inspection during operation has been developed and demonstrated in the lab scale and reported in the deliverable D2.1 and D2.2. Details about this technology will be described in Section 6 of this report as well.

To prove the USV based- imaging system can produce high quality images, a thorough testing plan was sketched (Table 1) and the associated risks were carefully evaluated. The preliminary test at GE's lab environment focused on the core system function and the remote controllability of all components. The test at the Mystic River aimed to test the overall system function, performance, and robustness in a representative water environment. The test in the ocean was to prove the feasibility of the USV-based imaging system for offshore wind blade inspection. Section 4.1 and Section 4.2 summarize the processes and key takeaways from the Mystic River and the Block Island wind farm test respectively.

Figure 17: An integrated system

Table 1: Field test plan

Test step	Objective	Status	Date	Risks	Risk impact level
Function test at GE Research after integration of USV and imaging system	Function test and remote screen sharing with AIS for environment monitoring	Completed	August 15	R1: Imaging system not compatible to the fixture on USV	Low
Factory Acceptance Testing at Mystic River Massachusetts Water Resources Authority (MWRA) wind turbine at the DeLauri Sewer Pump Station	testing system function, performance and robustness; acquire images for project risk abatement	Completed	Aug 22	R2: Imaging system damaged from river test ***(see alternative plan next page)***	***Medium***
Field testing at Block Island testing Launch USV from Block Island or other ports	Test system function and performance in real environment	Completed	Sep 2	R3: Water damage; system dysfunction due to the 4-hr commute in water; R4: Bad weather ***(See next page for alternative plan)***	**High**

4.1 Data Collection at the Mystic River

Mystic River is a 7.0-mile-long (11.3 km) river in Massachusetts. On the riverbank near the Massachusetts Water Resources Authority, there is a 1.5 megawatt wind turbine at the DeLauri Sewer Pump Station in Charlestown, Massachusetts. The team selected this site for the factory acceptance test for the integrated vessel to assess the system operability on the water and the imaging capability for wind blades.

As described in the deliverable D1.4, a plug-and-play fixture was designed to integrate the imaging system developed by GE with the USV from XOCEAN. Therefore, the installation time at the dock by the Mytic River was about 10 minutes with the USV in the water. The USV sailed to a location that was between 50 meters and 100 meters from a wind turbine situated on the riverbank (Figure 17). While the USV was in the water, a support vessel was nearby to monitor the USV for safety purposes. Two computer screens were set up on the support crew vessel to display images from the positioning camera and the inspection camera. Several camera settings were tried to find a balance between over or underexposing the image shots because of the changing sun direction, the white color of the blade, and the light blue background of the sky. For the inspection, the test team tried to get as close as possible to achieve the highest pixel resolution, while still giving a reasonable amount of white space in the images to be able to compensate for boat and blade movement. To get the best defect detail, the imaging system was pointed perpendicular to the blade surface as much as possible. Most of the pictures were taken when the blade was in the 6 o'clock or down position to reduce the shooting angle.

Our test team observed high quality pictures when objects were stationary or slow moving. Two exemplary pictures taken with the USV based imaging system are shown in Figure 18. Quantitative image assessment has been conducted in M4.2 to conclude whether the image quality is sufficient for defect recognition and meet the requirements.

From the river test, one area the team identified to improve was the video transmission interference. With both the positioning camera and the inspection camera next to each other on the imaging system, separating the two receivers with more distance or using another HDMI TX/RX system on a different band than 2.4Ghz could potentially reduce the interference.

Figure 18: Exemplary picture taken with the USV based imaging system.

(a) (b)

4.2 Data Collection in the Ocean

The Block Island Wind Farm is located 3.8 mi from Block Island, Rhode Island in the Atlantic Ocean. The five-turbine, 30 MW wind farm is owned by Ørsted US Offshore Wind and maintained by GE's Offshore Wind business unit. The ocean test of this project was conducted on the 2nd of September 2023, supported by GE's Offshore Wind team, and approved by Ørsted.

XOCEAN's USV departed from Point Judith, RI at 5am on the testing day. A crew boat accompanied the USV to the Block Island wind farm. At 3 knots, it took 4 hours for the USV to travel from RI to the Block Island port, New Shoreham. The GE team swiftly integrated the imaging system with the USV attributing to the plug-and-play fixture design. The USV and the crew boat then traveled to Block Island. Inside the crew boat's cabin, two HD screens, two HD video transmitters, a gimbal controller for aiming the blade and a remote shutter for image capturing were situated. Two GE researchers were well-coordinated on targeting the blade of interest and capturing the images. Figure 19 shows one of the GE's researchers controlling the shutter for image capturing, with the USV in the background, as well as a wide-angle view of the blade on the left screen, and a zoomed in version on the right.

Figure 19: Image capturing

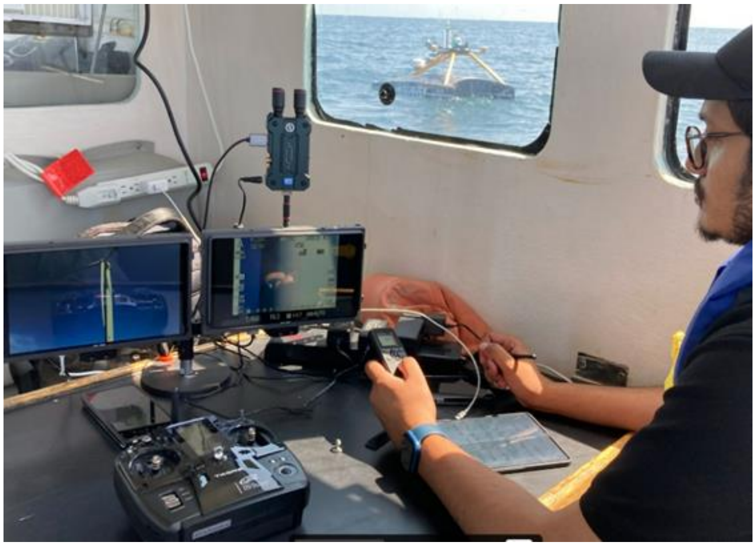

On the day of the testing, two of the five turbines at the wind farm were under maintenance which was beneficial for the team to test the imaging system capability without blade rotation. More than 1,500 pictures of two turbines, including the suction, pressure, leading edge and trailing edges surfaces were captured at an approximately 100 meters standoff distance from the blade. During the testing, the A.I.S team was on duty for environmental (marine life) observation, and remotely monitored for collision avoidance. The wave conditions during the 10-hour testing window are shown in

Figure 20. Although it was a moderate day based upon the wave condition, the recoded heave data on the USV still indicated the imaging system has experienced significant motion during the test.

Figure 20: Wave condition

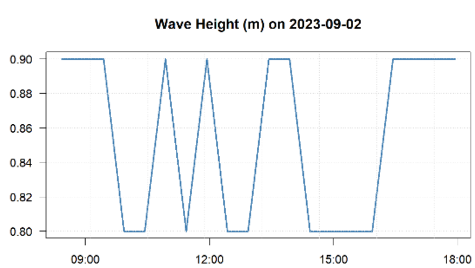

Figure 21: Heave data recorded on USV

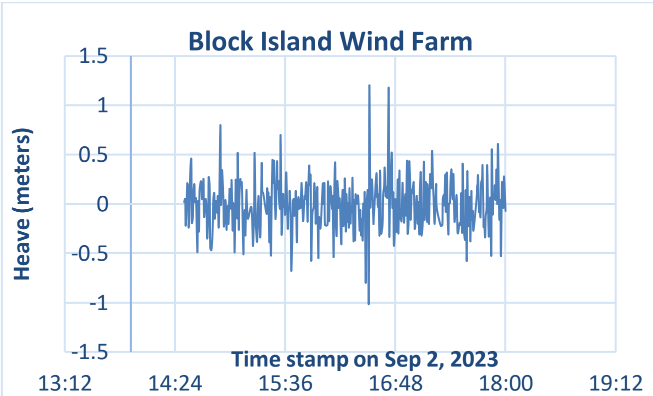

Figure 22: Pictures taken before and after camera setting optimization.

Through the test at the Block Island wind farm, the team proved the combined XOCEAN USV and GE imaging systems are able to take pictures in a representative offshore wind farm environment. The collected pictures mapped two blades fully, and we learned how to significantly optimize camera and gimbal settings. For example, the two pictures shown in Figure 22 were taken before and after the camera settings were optimized. Quantitative image quality assessment was reported in D4.2.

4.3 Vessel Strike Observation

While GE Global Research, in collaboration with XOCEAN, performed testing at the five (5) Block Island Wind Farm turbines, A.I.S was hired as the environmental observer during the entire transit and test. Figure 23 below illustrates the Wind Lease area and operational area. A team of two NMFS-approved Protected Species Observers (PSO) were provided by A.I.S., Inc. for remote monitoring operations. All PSOs attended a dedicated Monitoring and Mitigation training course prior to the beginning of survey operations. PSO training involved a detailed review of all relevant protected species compliance, data collection, and reporting conditions. A remote vessel strike avoidance watch was performed via real time video feeds from the visual cameras mounted on the USV during all periods of open water vessel transit for vessel strike avoidance mitigation implementation and documentation of protected species observations. Offshore operations for the XOCEAN-19 were remotely monitored for a total of 12 hours and 31 minutes. Figure 24 (below) illustrates this monitoring time. Because all remote monitoring occurred during daylight hours, only daylight visual observations was required, and no time was spent monitoring the thermal camera feeds. During the one-day test, no detections of marine protected species occurred, thus there was no need for implementation of vessel strike avoidance mitigation.

Figure 23: Map of the testing area.

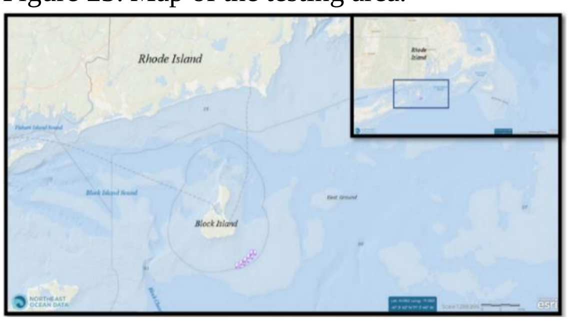

Figure 24: Remote monitoring effort by USV and observation type

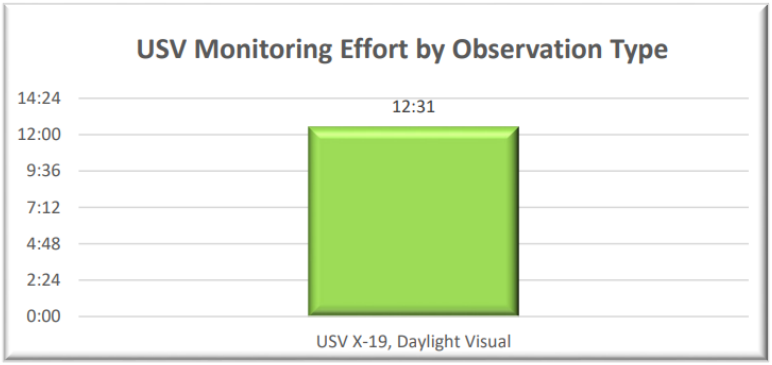

4.4 Conclusion of the Field Testing

In conclusion, the research team summarized the following key points from the ocean test:

- The overall system is well capable of producing RGB imagery consistent with the AI-based automated defect recognition for inspection purposes.
- A remote or automated control of the camera's settings is desirable to accommodate varying environmental conditions.
- 100m is about the right standoff to balance safety, the angle of attack and pixels per inch resolution for the purpose of inspections.
- The gimbal is more than capable of dealing with 1m swells and high frequency waves.
- Although the ocean test proved the USV based imaging system was effective for blade inspection in static or pinwheeling modes, integrating the automated blade tracking technology developed in Task 2 of this project will be critical to the USV based imaging system for fast spinning blades with a tip speed of tens or more than 100 meters per second.
- A purpose-built gimbal solution will need to be developed in next project phase to provide the following features.
    a. Environmental protection/lens wiper/cleaning
    b. Remote turn-on
    c. Securing statically for travel
    d. Cooling considerations
    e. Electro-mechanical integration with the USV

5 Data Quality Assessment

In Deliverable 2.1 and D2.2 we presented a pipeline for calibrating a two-camera system in a lab environment that can take high-resolution closeup images of a moving object and position the moving object back to the field-of-view (FOV) of the inspection camera (a.k.a tracking camera). To quantify the image quality and the effectiveness of positioning, the sharpness and the visible surface area (contour in pixel space) of the blade were employed as the metrics for quality assessment. In this milestone (M3.2), the same metrics were applied to assess the image quality of the field tests. The second parameter to calculate is the image resolution. As described in the conceptual design stage, a one-pixel-per-millimeter image resolution was desired at about 100-meter standoff distance. In addition, the ultimate objective of this project is to develop a novel method for offshore wind blade inspection. Therefore, the images acquired from the field tests were also assessed using GE's proprietary AI algorithms for defect detection.

The image sharpness and contour area calculation were summarized in Section 5.1. The image resolution estimation was reported in Section 0. The defect detection results using GE's AI algorithm pipeline were reported in Section 5.3.

5.1 Image Sharpness and Contour Area Calculation

The sharpness of each image was estimated using a focus score that was part of an autofocus method proposed by Herrmann et.al. [29]. To calculate the contour area, the blade was firstly detected with the Segment Anything Model (SAM), a new AI model by Meta, that can segment any object from an image [30]. And then the area of the blade was compared against the entire FOV. A higher value of sharpness and contour area indicates a better capture of the target blade.

We have analyzed some of the representative images taken from the leading edge, blade bottom facing downwards at different angles, and the pressure side. The best- and worst-case scenarios for each view of the blade has been summarized in Table 2:

Table 2: Best- and Worst-Case Scenarios for Sharpness and Contour Area (Block Island test)

	Best Case		**Worst Case**		**Sharpness**		**Contour Area**	
Blade View	**Sharpness**	**Contour Area**	**Sharpness**	**Contour Area**	**Mean**	**Std. Dev.**	**Mean**	**Std. Dev.**
Leading Edge	18.40	56335	79.56	253997	57.37	18.98	150709	63075.06
Pressure Side	15.50	47839	35.90	211344	23.16	5.23	113643.45	46319.66
Blade facing downwards	14.07	8481	45.89	172520	27.17	10.05	106326.78	38793.54

As can be seen through this analysis, the visible contour area affects the sharpness of the image. The range in the contour area is due to the movement of the camera from the tip (lowest visible surface) to the nacelle (thickest part of the blade). Higher values of sharpness and contour areas indicate better focus and resolution of the images.

Same calculation has been conducted for the images captured from the Mystic River, where the water motion on the testing day was very moderate so image quality was great as expected. The results were shown in Table 3.

Table 3: Best- and Worst-Case Scenarios for Sharpness and Contour Area (Mystic River test)

	Best Case		**Worst Case**					
Blade View	**Sharpness**	**Contour Area**	**Sharpness**	**Contour Area**	**Mean**	**Std. Dev.**	**Mean**	**Std. Dev.**
Leading Edge	4.13	40505	43.73	178876	19.88	11.79	101533.25	37828.17

5.2 Image Resolution Estimation

In the context of defect recognition, defects measurements are paramount to classify defects accurately. By determining the real-world size represented by each pixel, we can establish a direct relationship between the image and the physical world, ensuring that defects are identified with high precision and reliability. In the absence of actual 3D data, measuring a known feature's size within an image and dividing it by the total number of pixels can provide an alternative way to estimate the pixel resolution. Though pixel resolution is a function of geometry of the object, with planar assumption we can estimate rough order of magnitude pixel resolution from our images. Pixel resolution is also a function of directionality. Hence, in the absence of actual distance measurement between two known features along the length of the blade, we are only able to compute pixel resolution along the width of the blade using the length of the features divided by the total pixel numbers. Based upon approximation, we assumed the cross section showed in

Figure 25 is the widest section of the blade, which is 4.2 meters according to GE's Halide 150 turbine blade datasheet.

Figure 25: Illustration of pixel resolution calculation

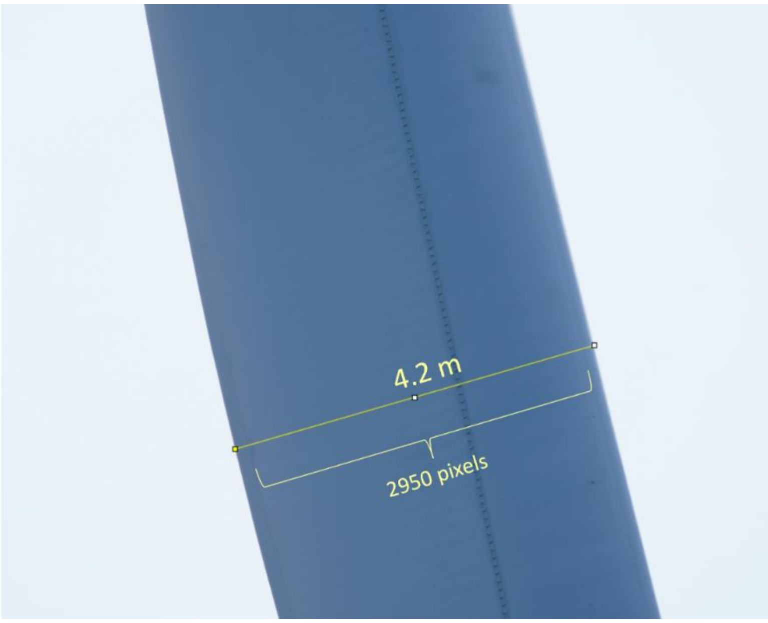

Therefore, in our analysis, we observed 0.06-inch pixel resolution which is extremely good for defect disposition and decisioning. Given that the standoff distance of the imaging system in the Block Island test was far more than 100 meters, we concluded the pixel resolution of our imaging system was in the ballpark of the design requirement.

5.3 Image Processing for Defect Detection

GE has developed a proprietary AI-based defect detection algorithm based on U-Net architecture [29] trained on data collected from onshore wind turbine. The U-Net architecture (Figure 26) has become a cornerstone in the field of computer vision and medical image analysis. This neural network architecture is particularly well-suited for tasks involving semantic segmentation, where the goal is to assign a class label to each pixel in an input image. U-Net's distinguishing feature is its U-shaped structure, which consists of a contracting path to capture context (Encoder) and a symmetric expanding path for precise localization (Decoder). The contracting path employs convolutional layers with progressively increasing receptive fields, enabling it to extract high-level features, while the expanding path uses transposed convolutions for up-sampling and generating pixel-wise predictions. Skip connections between corresponding layers in the contracting and expanding paths facilitate the transfer of fine-grained spatial information, aiding in accurate segmentation. U-Net's versatility and effectiveness have led to its widespread adoption in various applications, such as medical image segmentation, image-to-image translation, defect recognition and many more. Our AI algorithm is trained for detecting anomalies in the images (defect pixels vs background-pixels) and localize them. To identify the defect category associated with each anomaly, another neural network can be trained to classify these regions into defect classes.

We assessed the images collected from the field test and performed inference on the images using our AI algorithm. As can be seen in Figure 27, our algorithm was able to detect anomalies and localize them. In Figure 27, the red boxes represent anomalous regions for reviewing and disposition, the left column is the original images, and the right column is the AI predictions in red overlayed on the original images.

Performance can be further improved by fine-tuning the AI algorithm on the actual data from the offshore wind turbines. This demonstrates that the image quality and data distribution of defects in these images are similar to onshore wind and AI methods developed for on shore can be leveraged for human-assisted automated disposition.

Figure 26: U-Net architecture

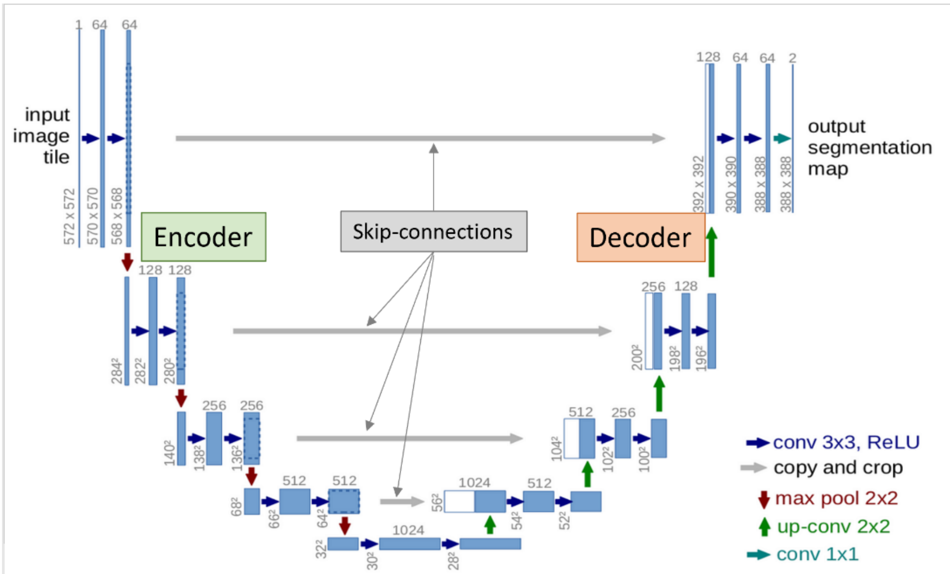

Figure 27: Example of AI-based detections of defects in images collected from the field test.

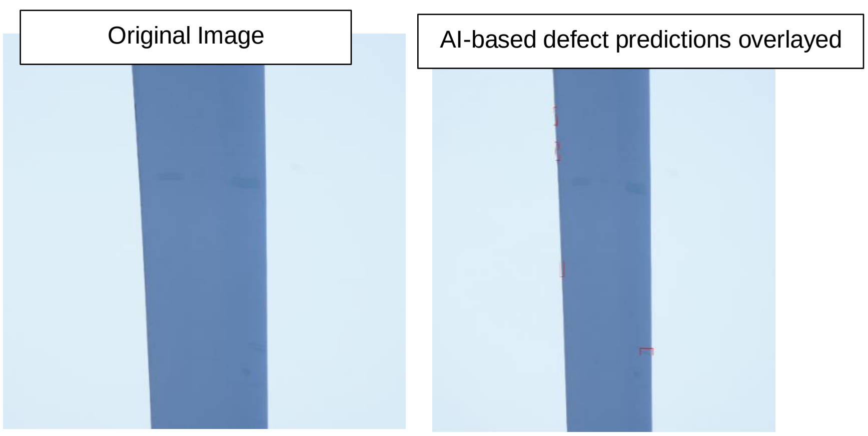

5.4 Conclusion for Data Quality Assessment

In this section, we have adopted four methods to process the images acquired from the field tests that include the image resolution, sharpness, contour area in pixel space, and image quality for defect detection. The objective was to prove the inspection images acquired using the USV based-imaging system have reasonable image quality to meet the inspection requirements for the offshore wind O&M. In summary, we have concluded that:

1) The field image sharpness from the ocean test is equivalent to the river test and lab test. This proved that our USV based images system is robust to capture high quality images in the ocean environment.

2) The approximate image pixel resolution meets the design but requires a more rigorous evaluation to establish pixel resolution at entire surface of the blade which would involve collecting calibrated 3D data with images.

3) Defect detection method developed for onshore imagery was able to generalize well for offshore data demonstrating that the images quality and data distribution is similar to onshore data and our AI methods can be leveraged for automated defect recognition and disposition.

6 Lab-based Feasibility Study on Low-latency Image Acquisition Control

6.1 Research Motivation for a Low-latency Image Acquisition

The focus of milestone 2.1 was to define a low-latency image acquisition system. The image acquisition system must be able to point the camera with enough precision and stability to reliably acquire the entire blade surface over the course of the inspection. Doing this offshore without the possibility for remote control requires that we develop a targeting system tolerant to the communication lag associated with offshore vessels. Lack of cellular coverage and the cost of direct satellite communication requires the need of an intelligent targeting system capable of data acquisition without direct human control over long missions for many turbines.

6.2 Design of the Low-latency Image Acquisition System

In order to capture high resolution images of the wind turbine blades and components, the image capturing system must be able to operate semi-autonomously on the surface vessel, with only periodic communication with the control center via the high-latency link. Figure 28 shows the overall system architecture of the proposed imaging system. It consists of cameras stabilized by a pan-tilt unit to capture images at the front-end. The back-end components consist of local storage and software modules that performs image processing and recognition, as well as turbine and blade tracking algorithms. A long-range or satellite wireless module will also be included for receiving parameters of targeted wind turbine models, and for uploading captured images when necessary.

Figure 28: Overall System architecture.

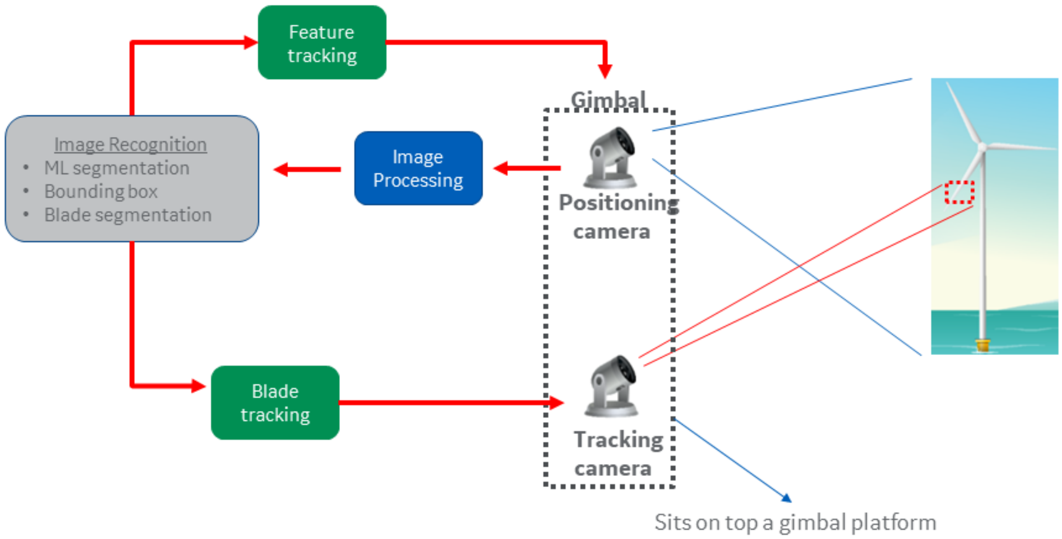

6.3 Calibration Pipeline

A pipeline for calibrating a two-camera system (Figure 29) in a lab environment has been successfully created that can take high-resolution closeup images of a moving object with reasonable speed and accuracy. The first camera (PC) is a low-resolution, wide-angle camera for positioning the platform and spotting. The second camera (TC) is a high-resolution camera with a zoom lens, used for tracking the position of root/mid/tip section of a blade, and take burst photos of fixed points on the blades or follow a spiral motion path to track each blade. A pan-tilt unit (PTU) has been used to keep the tracked blade at the center of the frame of the second camera. An augmented reality (AR) tag-based tracking algorithm is used for calibrating the offset between the location of the tracked object on the wide-angle camera frame, and the pan and tilt combinations of the PTU that keeps the tracked object in frame for the zoom-lens camera.

Figure 29: Camera setup for benchtop tests

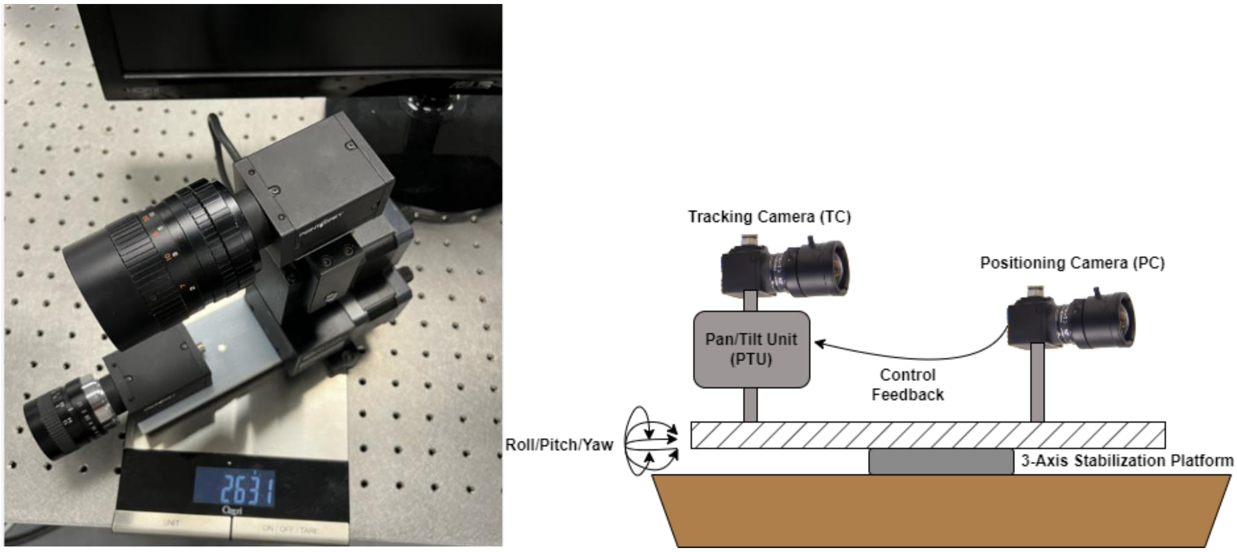

6.4 Testing the Tracking Algorithm

In Deliverable 2.1, we presented a pipeline for calibrating a two-camera system in a lab environment that can take high-resolution closeup images of a moving object with reasonable speed and accuracy. In Deliverable 2.2, we present the actual tracking algorithm, a set of benchtop tests, and some metrics using which we evaluated the proficiency of our method.

6.5 Conclusion of the Lab-based Tracking System

In the lab-based simulations for feasibility study on calibrating the two-camera system for high quality and accurate image acquisition, we have developed and optimized a custom trained Convoluted Neural Network (CNN)-based object detection model to detect all three blades and the nacelle of the turbine. To simulate the motions from the real environment, we applied the motion of a robot arm to simulate the actual wave motion similar to the Atlantic Ocean, and then tested the calibration method and stabilization algorithm of the two-camera system. Based upon our study, we have proved that the blade location can be predicted and updated in real time so the TC can capture high quality images while the blade is rotating.

As future effort in the future project, this system will be tested in a real-world scenario by mounting it on an autonomous surface vessel and inspecting offshore turbine blades.

7 Summary and Next Steps

In this project, the team successfully integrated an USV based-, dual camera-, imaging system capable of capturing high quality images in a range of 50 meters to 150 meters for offshore wind turbines. Even with uncertainties from the weather forecast, complicated logistics to arrange transportation and crew vessels, and careful coordination among a multiple-institute team, this system was tested in both river and ocean environment. Through the test at the Block Island wind farm, the team has concluded that the USV based imaging system can be potentiality employed to inspect wind turbine blades, at a safe distance, and generate high quality images.

Regarding quantitative image quality assessment, the team adopted four metrics: image sharpness, contour areas, image resolution, and defect detectability using AI algorithm. The first three parameters were calculated for representative images acquired from the field tests that includes the different sections of wind turbine blades. The image quality is equivalent to the quality of other inspection modality such as drone.

To prove the inspection images acquired using the USV based- imaging system have a reasonable image quality for defect detection, the team has ran GE's proprietary defect detection AI algorithm developed for onshore wind O&M. The algorithm was successful in detecting defects on the images. The defect detection method developed for on shore imagery was able to generalize well for offshore data demonstrating that the images quality and data distribution from our field test is similar to onshore data and AI methods can be leveraged for automated defect recognition and disposition.

To realize real time blade tracking and position imaging camera to a proper FOV, a lab based-, small scale prototype was developed, and a tracking AI pipeline was proved to be capable of re-positioning the imaging camera for better image quality. However, this blade tracking solution needs to be proved at a full-scale on a real offshore wind turbine and integrated to the full-scale imaging system described in Section 3 .

As the future plan, if there is a potential Phase II project opportunity, the team will propose a full-scale POC systema and demonstration and advance the technology to TRL7.

Reference

1. Global Wind Energy Council, “Global Wind Report 2018,” April2019.
2. Department of Energy, “Offshore Wind Market Report: 2021 Edition,” August 2021.
3. The White House, “Executive Order on America’s Supply Chains.” Washington, D.C., 2021: https://www.whitehouse.gov/briefing-room/presidential-actions/2021/02/24/executive-order-on-americas-supply-chains/
4. Stehly and Beiter P.,“2018 Cost of Wind Energy Review,” National Renewable Energy Lab, Golden, CO, 2020.
5. Global costs analysis -the year offshore wind costs fell, Wind Power Monthly: https://www.windpowermonthly.com/article/1380738/global-costs-analysis-year-offshore-wind-costs-fell
6. D. R. Ahuja and M. Tatsutani, "Sustainable energy for developing countries,", 2009. [Online]. Available: https://journals.openedition.org/sapiens/823. [Accessed 15 12 2022].
7. J. S. Logan and S. M. Kaplan, "Wind Power in the United States: Technology, Economic, and Policy Issues,", 2008. [Online]. Available: https://fas.org/sgp/crs/misc/rl34546.pdf. [Accessed 15 12 2022].
8. A. Farley, "The Challenges of Implementing Evidence Based Practice: Ethical Considerations in Practice, Education, Policy, and Research," *Social work and society,* vol. 7, no. 2, pp. 246-259, 2009.
9. D. Zhang, K. Burnham, L. Mcdonald, C. MacLeod, G. Dobie, R. Summan and G. Pierce, "Remote inspection of wind turbine blades using UAV with photogrammetry payload," , 2017. [Online]. Available: https://strathprints.strath.ac.uk/63321. [Accessed 13 12 2022].
10. L. Wallace, A. Lucieer, D. Turner and C. Watson, "Error assessment and mitigation for hyper-temporal UAV-borne LiDAR surveys of forest inventory.,", 2011. [Online]. Available: http://locuscor.net/silvilaser2011/papers/033_wallace.pdf. [Accessed 19 12 2022].
11. B. J. Michini and F. Blanc-paques, "UNMANNED AERIAL VEHICLE WIND TURBINE INSPECTION SYSTEMS AND METHODS,", 2018. [Online]. Available: https://patentimages.storage.googleapis.com/58/3a/ca/5b552b4aab06e4/us20180003161a1.pdf. [Accessed 13 12 2022].
12. B. Schäfer, D. Picchi, T. Engelhardt and D. Abel, "Multicopter unmanned aerial vehicle for automated inspection of wind turbines,", 2016. [Online]. Available: https://ieeexplore.ieee.org/document/7536055. [Accessed 13 12 2022].
13. A. Shihavuddin and X. Chen, "DTU - Drone inspection images of wind turbine,", 2018. [Online]. Available: https://data.mendeley.com/datasets/hd96prn3nc/2. [Accessed 14 12 2022].
14. A. Shihavuddin, X. Chen, V. Fedorov, A. Christensen, N. A. B. Riis, K. Branner, A. B. Dahl and R. R. Paulsen, "Wind Turbine Surface Damage Detection by Deep Learning Aided Drone Inspection Analysis," *Energies,* vol. 12, no. 4, p. 676, 2019.
15. P. D. Løhndorf, D. O. Arroyo and Z. Yang, "LiDAR Assisted Camera Inspection of Wind Turbines: Experimental Study,", 2019. [Online]. Available: https://vbn.aau.dk/da/publications/lidar-assisted-camera-inspection-of-wind-turbines-experimental-st. [Accessed 13 12 2022].

16. P. Durdevic, D. Ortiz-Arroyo, S. Li and Z. Yang, "Vision aided navigation of a quad-rotor for autonomous wind-farm inspection," *IFAC-PapersOnLine,* vol. 52, no. 8, pp. 61--66, 2019.
17. G. Papadopoulos, H. Kurniawati, A. S. B. M. Shariff, L. J. Wong and N. M. Patrikalakis, "Experiments on surface reconstruction for partially submerged marine structures," *Journal of field robotics,* vol. 31, no. 2, pp. 225-244, 2014.
18. F. Shkurti, A. Xu, M. Meghjani, J. C. G. Higuera, Y. Girdhar, P. Giguère, B. B. Dey, J. Li, A. Kalmbach, C. Prahacs, K. Turgeon, I. Rekleitis and G. Dudek, "Multi-domain monitoring of marine environments using a heterogeneous robot team,", 2012. [Online]. Available: http://cim.mcgill.ca/~florian/pdfs/iros12_0567_fi.pdf. [Accessed 20 12 2022].
19. A. M. Pinto *et al*., "ATLANTIS - The Atlantic Testing Platform for Maritime Robotics," *OCEANS 2021: San Diego – Porto*, 2021, pp. 1-5, doi: 10.23919/OCEANS44145.2021.9706059.
20. D. F. Campos, A. Matos and A. M. Pinto, "Modular Multi-Domain Aware Autonomous Surface Vehicle for Inspection," in *IEEE Access*, vol. 10, pp. 113355-113375, 2022, doi: 10.1109/ACCESS.2022.3217504.
21. P. Tavner, J. Xiang and F. Spinato, "Reliability analysis for wind turbines," *Wind Energy,* vol. 10, no. 1, pp. 1-18, 2007.
22. A. Kulsinskas, P. Durdevic and D. Ortiz-Arroyo, "Internal Wind Turbine Blade Inspections Using UAVs: Analysis and Design Issues," *Energies,* vol. 14, no. 2, p. 294, 2021.
23. K. Fischer, T. Stalin, H. Ramberg, J. Wenske, G. Wetter, R. Karlsson and T. Thiringer, "Field-Experience Based Root-Cause Analysis of Power-Converter Failure in Wind Turbines," *IEEE Transactions on Power Electronics,* vol. 30, no. 5, pp. 2481-2492, 2015.
24. I. Cotton, N. Jenkins and K. Pandiaraj, "Lightning protection for wind turbine blades and bearings," *Wind Energy,* vol. 4, no. 1, pp. 23-37, 2001.
25. V. C. Igwemezie, A. Mehmanparast and A. Kolios, "Materials selection for XL wind turbine support structures: a corrosion-fatigue perspective," *Marine Structures,* vol. 61, no., pp. 381-397, 2018.
26. G. Fiore and M. S. Selig, "Simulation of Damage for Wind Turbine Blades Due to Airborne Particles," *Wind Engineering,* vol. 39, no. 4, pp. 399-418, 2015.
27. A. Juengert and C. Grosse, "Inspection techniques for wind turbine blades using ultrasound and sound waves," *Proceedings of the NDTCE,* vol. 9, 2009.
28. A. Kulsinskas, P. Durdevic and D. Ortiz-Arroyo, "Internal wind turbine blade inspections using UAVs: Analysis and design issues," *Energies,* vol. 14, no. 2, p. 294, 2021.
29. O. Ronneberger, P. Fischer , T. Brox, “U-Net: Convolutional Networks for Biomedical Image Segmentation“, Medical Image Computing and Computer-Assisted Intervention – MICCAI 2015, Volume 9351, 2015
30. C. Herrmann, R. Strong Bowen, N Wadhwa, “learning to autofocus”, CVPR, 2020.